

# Moment capacity of cast-iron beams exposed to fire

**1 Chrysanthos Maraveas** Dipl.Eng., MSc, MSc, DIC, PhD, CEng, MICE  
University of Manchester, Manchester, UK  
(corresponding author: c.maraveas@maraveas.gr)

**2 Yong C. Wang** BEng, PhD, CEng, FIStructE  
Professor, University of Manchester, Manchester, UK

**3 Thomas Swailes** BEng, MICE, MIStructE, CEng  
Lecturer, University of Manchester, Manchester, UK



Cast-iron girders were used in many nineteenth century structures, especially in fireproof flooring systems (such as jack arches). Many such structures are still in use today and it is important that they fulfil the current requirements on fire resistance when there is a change of use. Cast iron has limited ductility so it is not possible for cast-iron beams to achieve total plasticity as for modern steel beams. Furthermore, cast iron has different mechanical properties in tension and compression and there is often a severe non-uniform temperature distribution in cast-iron beam sections. This paper presents the development of a simplified method to calculate the bending moment capacity of cast-iron beams in a jack arched system exposed to a standard ISO 834 fire. The method is based on an assumed strain distribution in the cross-section. A comparison of the results calculated using the simplified method with those using the fibre method, validated by Abaqus simulation results, indicates that the proposed simplified method is sufficiently accurate as the basis of a design method.

## Notation

$F_c$	compressive force
$F_t$	tensile force
$f_y$	yield strength
$k$	curvature
$M$	moment
$M_{el,Rd}$	design moment resistance
$M_{fi}$	applied bending moment in fire situation
$T$	temperature
$t$	fire exposure time
$W_{el,u}$	tensile elastic modulus
$y$	distance from bottom of cross-section
$y_{CG}$	distance of centre of gravity from bottom of cross-section
$\gamma_d$	ambient temperature design safety factor
$\gamma_{fi}$	safety factor for fire design
$\varepsilon$	strain
$\mu$	utilisation factor
$\sigma$	stress

columns, cast iron was also used in beams for more than 70 years, especially during the period 1820–1850 (IStructE, 1996). Cast-iron beams were partially fire protected by means of various types of thermal insulation systems (Hurst, 1990; Swailes, 2003; Wermiel, 1993), with the jack arch floor (Figure 1) being the most widely applied. However, because of the limited use of cast-iron structures in modern construction, there has been very limited research on cast-iron structures, with most of the relevant research studies being focused on renovation (Friedman, 1995; Parmenter, 1996; Paulson *et al.*, 1996; Rondal and Rasmussen, 2003; Swailes, 1995).

This paper deals with cast-iron beams exposed to fire. Cast-iron structural beams exhibit different behaviour from that of modern steel beams. When cast-iron beams are used as part of jack arched construction, the temperature distribution in the cast-iron cross-section is extremely non-uniform. In addition, the stress–strain curve of cast iron does not possess the degree of plastic behaviour of steel, making it not possible to analyse cast-iron beams based on the plastic analysis method. Furthermore, cast iron shows different behaviour under tension and compression (Angus, 1976; Kattus and McPerson, 1959; Maraveas *et al.*, 2015; Palmer, 1970). As a result, the plastic bending moment capacity method for steel beams, which is the

## 1. Introduction

Many nineteenth century historic buildings throughout the UK, central and western Europe as well as the USA were built using cast-iron structural elements. Besides wide usage in

Offprint provided courtesy of [www.icevirtuallibrary.com](http://www.icevirtuallibrary.com)  
Author copy for personal use, not for distribution

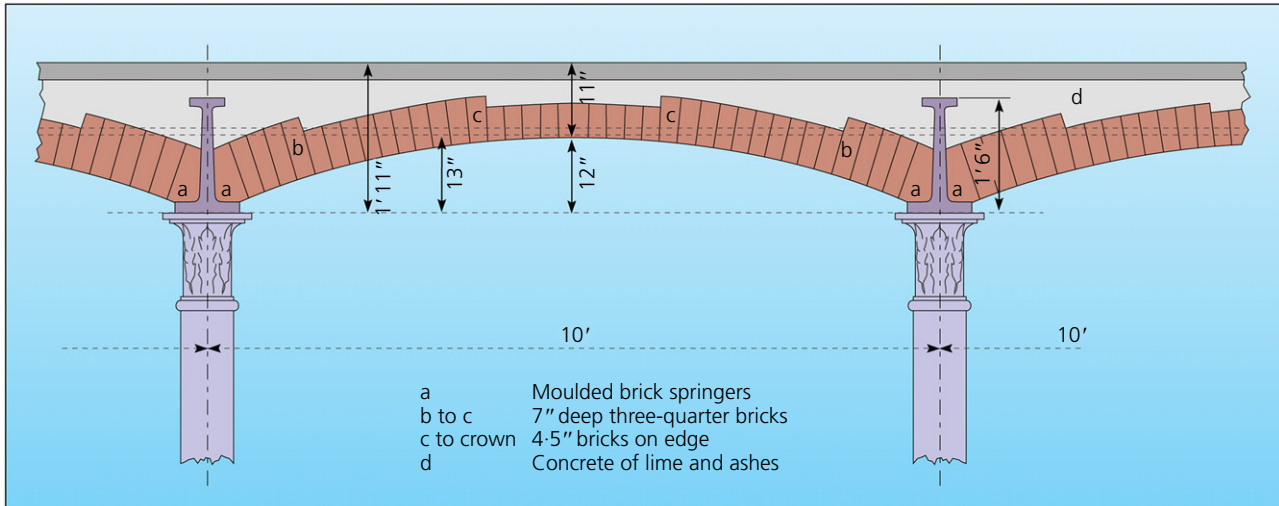


Figure 1. Typical jack arch flooring system (Swailes, 2003);  
1"  $\approx$  2.5 cm; 1'  $\approx$  30 cm

basis of fire resistance design methods for steel beams, is not applicable to cast-iron beams.

It is thus necessary to develop a different calculation method for cast-iron beams exposed to fire. A possible approach is to adapt a strain-based approach, similar to the work of Angus (1976), Clark (1901) and Bodzak *et al.* (2014) at ambient temperature. In this method, the strain distribution in the cast-iron cross-section is defined. Based on this, the stress distribution is calculated, which can then be used to obtain the bending moment capacity of the cast-iron beam. A strain-based approach is developed in this paper. The development procedure is as follows.

- The thermal profiles (temperature distributions) in the cast-iron cross-section of a typical unprotected are calculated using numerical modelling.
- The moment capacities of the cast-iron beams are calculated with a fibre analysis model. This fibre analysis method, which is used because it is very quick to execute, is compared with numerical simulation results using Abaqus for validation.
- The fibre analysis results are then used to check the various key assumptions in the strain-based bending moment capacity method.

In these calculations, the thermal and mechanical properties at elevated temperatures of the various materials of jack arched construction are based on work reported by Maraveas *et al.* (2013, 2014, 2015).

This paper considers both unprotected beams (i.e. fire exposure to the entire perimeter of the cross-section, see Figure 2) and protected beams (i.e. jack arched, with only the bottom flange

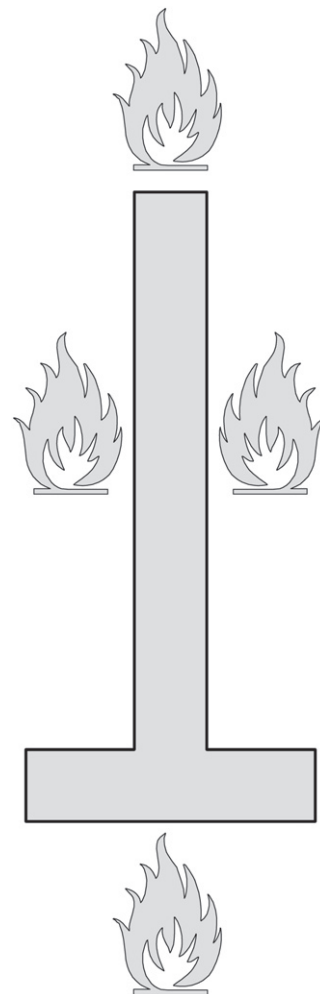


Figure 2. Unprotected cross-section exposed to fire

Offprint provided courtesy of www.icevirtualibrary.com  
Author copy for personal use, not for distribution

exposed to fire). Unprotected cast-iron beams were sometimes used to support types of floor covering other than brickwork jack arches, for example stone slabs or timber boards. Occasionally, unprotected primary cast-iron beams are found supporting partially protected secondary cast-iron joists. Cast-iron beams may be left unprotected either temporarily during renovation or permanently as part of a refurbishment in which the jack arch system is locally removed for the insertion of a new staircase or the creation of an area with double floor height.

Due to non-uniform temperature distributions in cast-iron beams, thermal strains and thermal stresses can develop in the cross-sections. As will be shown later in the paper, large portions of a cast-iron cross-section reach full yield in tension and compression in the outer fibres that contribute the majority of bending resistance to the cross-section. The effects of thermal strain and thermal stress are negligible, as in conventional steel beams that reach their plastic bending moment resistances. For simplicity, the effects of thermal strain and thermal stress are not considered in this paper.

## 2. Fibre analysis model and validation against finite-element results

The fibre analysis model, also referred to as the moment–curvature method, is based on the work of Burgess *et al.* (1988, 1990) but does not account for thermal expansion. Referring to Figure 3, which shows a cross-section with curvature  $k$  and corresponding strain and stress distributions, the method is summarised as follows.

- The initial position of the neutral axis is assumed to be at the centre of gravity.
- The cross-section is divided into a large number of fine layers.
- The strain at the mid-depth of each layer is calculated.

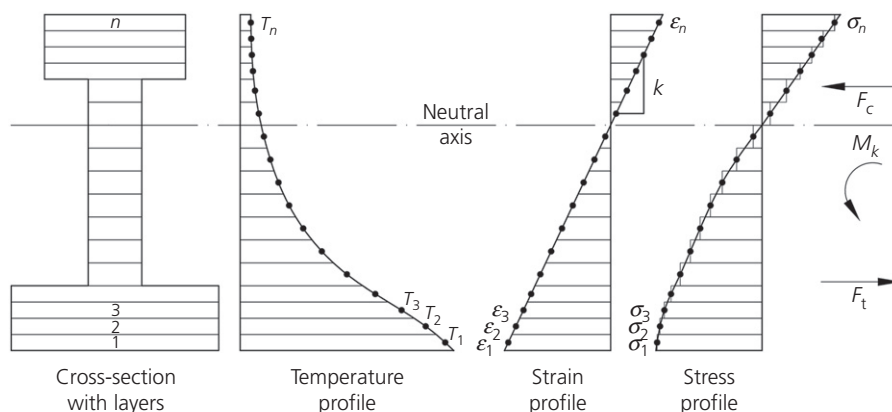


Figure 3. Fibre model: cross-section with curvature  $k$  and corresponding strain and stress distributions

- The temperature at the mid-depth of each layer is calculated.
- The stress at the mid-depth of each layer is calculated.
- The force of each layer is calculated.
- The tensile ( $F_t$ ) and compressive forces ( $F_c$ ) of all layers are summed.
- If  $|F_t - F_c|/F_t < r$ , where  $r$  is a small value (taken as 0.001 in this research), the corresponding moment ( $M$ ) is calculated.
- If  $|F_t - F_c|/F_t > r$ , the algorithm returns to step 1 and the position of the neutral axis is modified according to the equation  $y_{n+1} = y_n - [(F_t - F_c)/(F_t + F_c)] \times y_{CG}$  (where  $y$  is the distance from the bottom of the cross-section and  $y_{CG}$  is the distance of the centre of gravity from the bottom of the cross-section).
- If increasing the curvature gives a smaller bending moment, then the ( $M, k$ ) result of the previous iteration is the first point of the descending branch of the moment–curvature curve, and the bending moment is the final bending moment capacity of the beam.

Figure 20 (Appendix I) shows the results of a typical converged iteration of calculations.

For validation of the fibre analysis method, a finite-element model, using the general-purpose software Abaqus, was created. Figure 4 shows the materials and dimensions of the structure, based on Swailes (1995). The standard ISO 834 fire condition was used (ISO, 1999). The heat transfer boundary conditions were according to EN 1993-1-2 (CEN, 2005a): at the exposed surface, the convective heat transfer coefficient was  $25 \text{ W/m}^2\text{K}$  and the resultant emissivity value was 0.7; the total heat transfer coefficient for the unexposed surface was assumed to have a value of  $9 \text{ W/m}^2\text{K}$ . The heat transfer analysis was carried out for a total duration 120 min. Two

Offprint provided courtesy of www.icevirtuallibrary.com  
Author copy for personal use, not for distribution

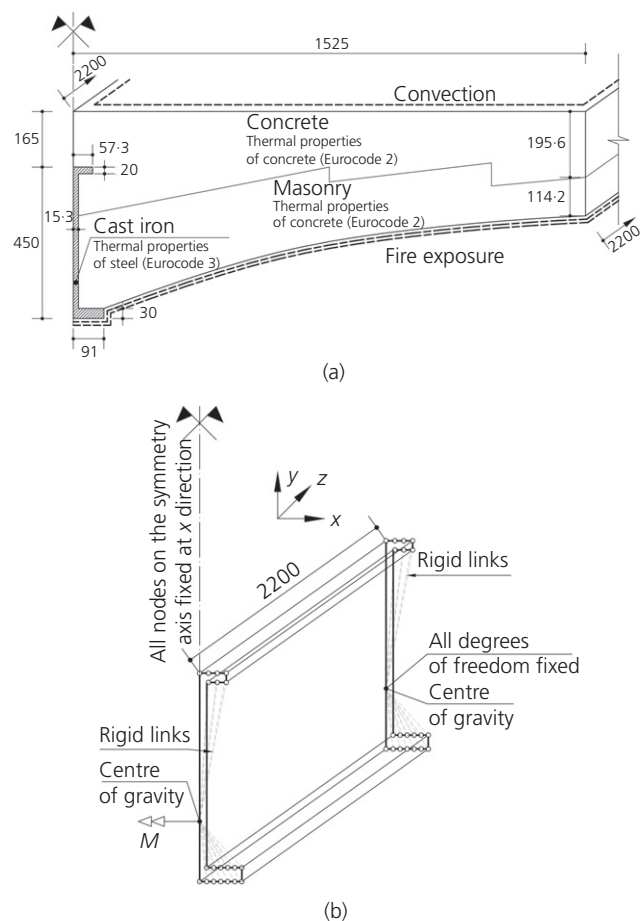


**Figure 4.** Geometry, dimensions, materials and boundary conditions of (a) the thermal analysis model and (b) the structural analysis model (dimensions in mm)

types of stress–strain–temperature ( $\sigma$ – $\epsilon$ – $T$ ) relationships were used – one with symmetrical compressive and tensile behaviour and the other with the actual  $\sigma$ – $\epsilon$ – $T$  diagram for cast iron according to Maraveas *et al.* (2015). Figure 5 shows the two types of assumed  $\sigma$ – $\epsilon$ – $T$  relationships.

Figure 6 compares the finite-element analysis results with the results obtained from the fibre model for the two types of  $\sigma$ – $\epsilon$ – $T$  relationships for fire exposures of 0, 60 min and 120 min. The agreement is very good, suggesting that the fibre model can be used in further parametric study for developing the simplified analysis method. Some minor differences between the two models are expected because

- the finite-element model simulates a beam and the fibre model analyses a cross-section; the beam model considers deformations of the cross-section
- the finite-element model considers more refined temperature and stress distributions.

### 3. Parametric study results

The fibre analysis method described in the previous section was used to conduct a parametric study to obtain the bending moment capacities of different types of cast-iron sections. The investigated parameters were

- the cross-section factor, which is function of the thickness of the bottom flange and the exposed surface
- the web thickness, which affects the temperatures developed in the web
- the height of the cross-section as this influences the thermal gradient.

Four types of cast-iron cross-sections were analysed. These were based on the work of Fitzgerald (1988) and are shown in Figure 7. The stress–strain–temperature relationships used were based on the work of Maraveas *et al.* (2015), as shown in Figure 5(b).

### 4. Cross-section temperatures

Thermal analyses were conducted to determine the temperature profiles of the unprotected as well as the partially protected (jack arch system) systems. The temperature study was carried out via two-dimensional heat transfer analysis using the commercial software Abaqus. The thermal properties of cast iron were assumed to be those of steel, as defined in EN 1993-1-2 (CEN, 2005a). This assumption was proposed by Maraveas *et al.* (2013) and has been proven to give satisfactory results (Maraveas *et al.*, 2014). Moreover, for jack arched systems, early concrete and masonry were modelled according to the thermal properties of modern concrete as per EN 1992-1-2 (CEN, 2005b), using the lower bound thermal conductivity values as suggested by Maraveas *et al.* (2015).

#### 4.1 Thermal profiles of partially protected cross-sections

Figure 8 shows the temperature distributions in the four types of cast-iron cross-section at different fire exposure times. As expected, owing to the presence of insulation materials, there are very high thermal gradients.

#### 4.2 Temperatures of unprotected cast-iron cross-sections exposed to ISO fire

The temperature evolution in the unprotected sections depends on their thickness. However, the variation in temperature in the unprotected section, as typified in Figure 9(a), is small. Therefore, uniform temperature may be assumed and the average temperature may be used. Figure 9(b) shows the average temperature–time relationships used for the four different unprotected cast-iron beams.

### 5. Moment capacities from fibre analysis

Figure 10 shows the calculated reductions of moment capacities of the different structures, with or without

Offprint provided courtesy of [www.icevirtualibrary.com](http://www.icevirtualibrary.com)  
Author copy for personal use, not for distribution

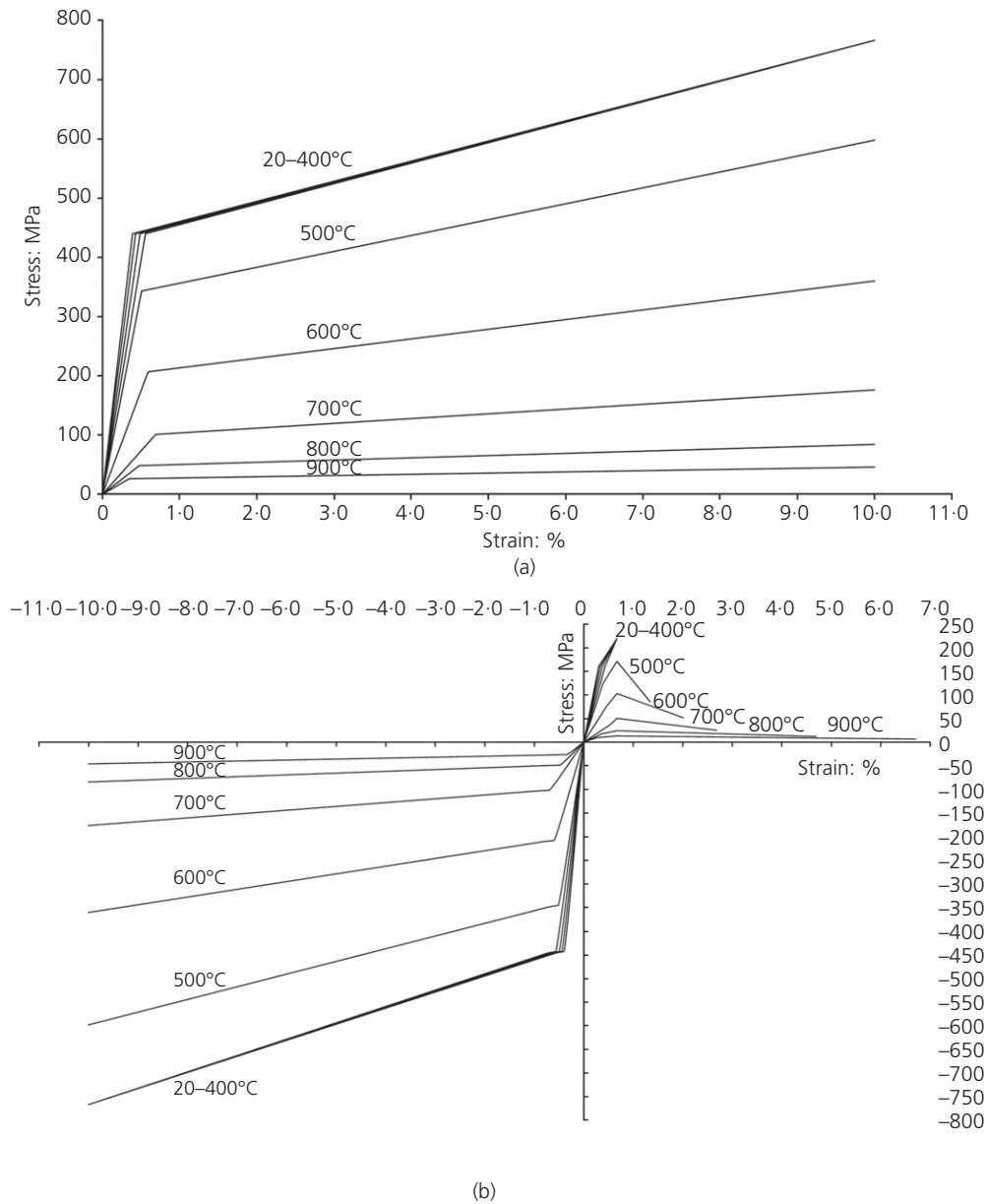


**Figure 5.** Two types of stress-strain-temperature ( $\sigma$ - $\epsilon$ - $T$ ) relationships: (a) with symmetrical compressive and tensile behaviour; (b) with  $\sigma$ - $\epsilon$ - $T$  diagrams for cast iron according to Maraveas *et al.* (2015)

protection, as a function of the standard fire exposure time. Figure 10 also shows (indicated by the horizontal lines) the approximate utilisation factors, defined as the ratio of the applied moment under the fire condition for the different structures. Appendix 2 uses an example to show how the utilisation factor is calculated. It can be seen that the fire resistances of these structures are quite high ( $>R60$ ). Indeed, if the design load is calculated according to the London County Council (General Powers) Act 1909 (1909), a fire resistance rating of

$R120$  may be achieved. This indicates that cast-iron structures should usually have sufficient fire resistance. Of course, in the above assessment, the applied load in fire is low because, historically, cast-iron structures were designed with high safety factors due to a lack of certainty regarding their mechanical properties and construction. In future assessments of cast-iron structures, it is possible that more refined understanding may lead to reduced safety factors and hence higher applied load (utilisation factor) and lower fire resistance. Careful assessment

Offprint provided courtesy of [www.icevirtuallibrary.com](http://www.icevirtuallibrary.com)  
Author copy for personal use, not for distribution

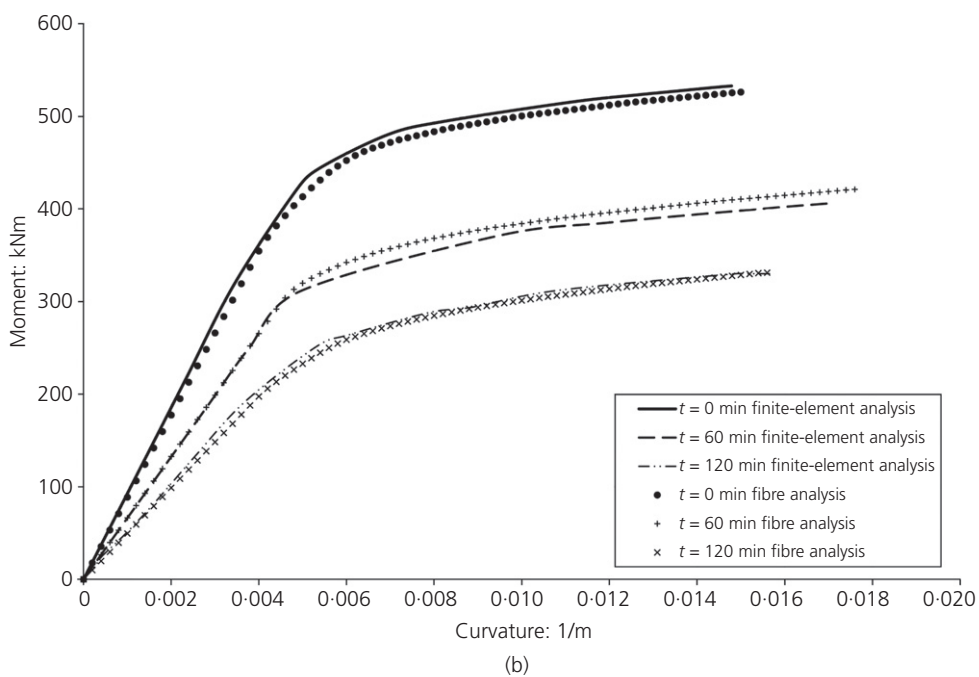
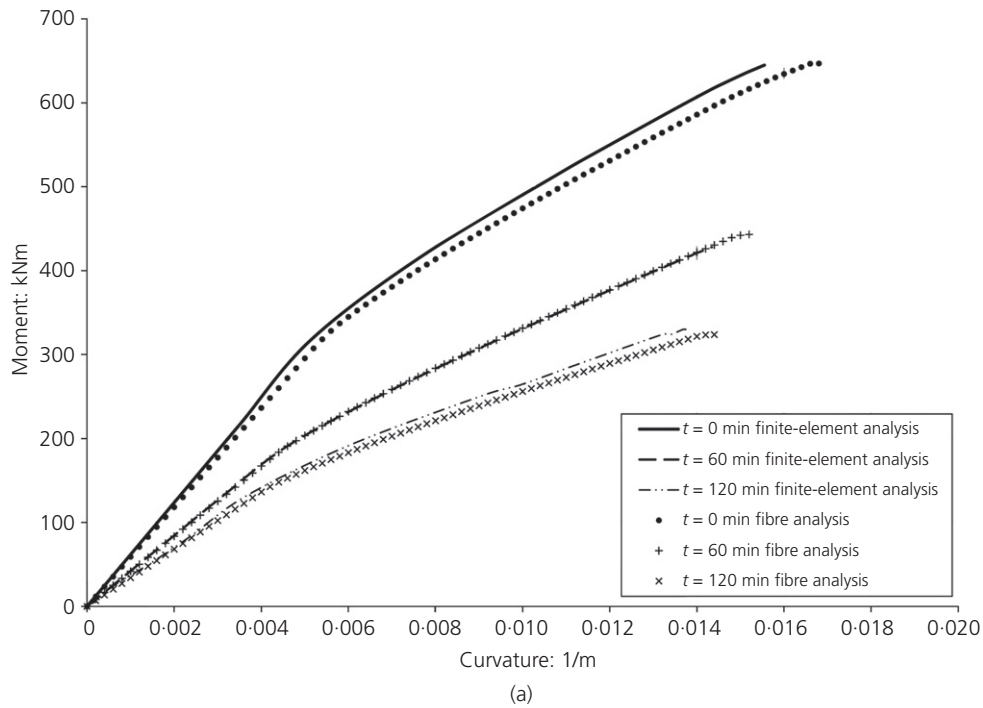


**Figure 6.** Comparison of Abaqus simulation and fibre analysis results: (a) for non-symmetric stress-strain-temperature ( $\sigma$ - $\epsilon$ - $T$ ) relationships (Maraveas *et al.*, 2015); (b) for symmetric  $\sigma$ - $\epsilon$ - $T$  relationships

Offprint provided courtesy of www.icevirtualibrary.com  
Author copy for personal use, not for distribution

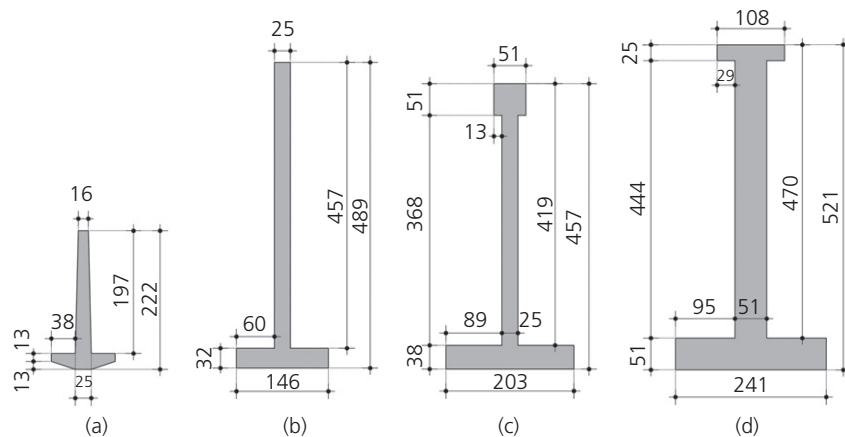


**Figure 7.** Cast-iron cross-section types used in parametric study (based on Fitzgerald (1988)): (a) Marshall mill (1817), jack arch span 3.35 m; (b) Armlay mill (1823), jack arch span 2.60 m;

(c) Shaw's G mill (1851), jack arch span 2.44 m; (d) Shaw's H mill (1880), jack arch span 2.75 m (dimensions in mm)

of the fire resistances of cast-iron beams would then be required and the purpose of developing a simplified method is to enable this assessment.

## 6. Simplified methods of calculating the moment capacities of cast-iron beams

### 6.1 Unprotected cross-sections

For a uniform temperature, the change in cast-iron beam bending moment resistance will be governed by the reduction in cast-iron tensile strength because the tensile strength of cast iron is lower than the compressive strength (Angus, 1976; Maraveas *et al.*, 2015). This is confirmed in Figure 11, which compares the residual cast-iron strength reduction factor with the cast-iron tensile strength reduction factor at elevated temperatures. The two sets of curves practically coincide. The slightly higher reduction at temperatures around 400°C is a result of the reduction in Young's modulus. Since the applied bending moments are likely to be much lower than the residual bending moment resistance at around 400°C, the cast-iron temperature will be much higher and the small differences at temperatures around 400°C are considered insignificant.

### 6.2 Partially protected cast-iron beams

#### 6.2.1 Simplified method of calculating temperature profiles

In order to simplify calculations of the thermal profiles of partially protected cast-iron beams, the method suggested by Zaharia and Franssen (2012) for slim floors can be used. Although this method uses slightly different thermal analysis parameters (based on the proposed values of EN 1993-1-2 (CEN, 2005a) and EN 1992-1-2 (CEN, 2005b)) and the upper

bound thermal conductivity of concrete, the differences between the temperature profiles of the present work and the equations proposed by Zaharia and Franssen (2012) are moderate, as shown in Figure 12. The effects of using the simplified temperature profiles will be assessed in Section 6.2.2.

#### 6.2.2 Strain profiles

The proposed method for calculating the bending moment capacity of a cast-iron beam is based on a strain approach. Figure 13 shows the maximum tensile and compressive strains in the different beams as a function of the average temperature in the bottom (tensile) flange. It can be seen that both maximum strains are grouped together within a very narrow band. At lower temperatures, the maximum tensile strain is close to 0.67%, this being the tensile strain at peak tensile stress, as shown in Figure 5(b). At higher temperatures, although the tensile strain at tensile peak stress is still 0.67%, because the stress at higher strain is close to the peak stress, higher maximum strains at the edge of the bottom flange can develop to allow the inner cast iron to develop high stresses. For the development of a simplified bending moment capacity calculation method for cast-iron beams, it is possible to give approximate maximum tensile and compressive strain-temperature relationships.

The approximate maximum tensile and compressive strain-tensile flange temperature relationships are

$$1. \quad \begin{aligned} \varepsilon_{t,T} &= \varepsilon_{t,20} & 20^\circ\text{C} \leq T \leq 400^\circ\text{C} \\ \varepsilon_{t,T} &= \varepsilon_{t,20} + 0.6 \left( \frac{T - 400}{500} \right) \varepsilon_{t,20} & 400^\circ\text{C} < T \leq 900^\circ\text{C} \end{aligned}$$

Offprint provided courtesy of www.icevirtuallibrary.com  
 Author copy for personal use, not for distribution

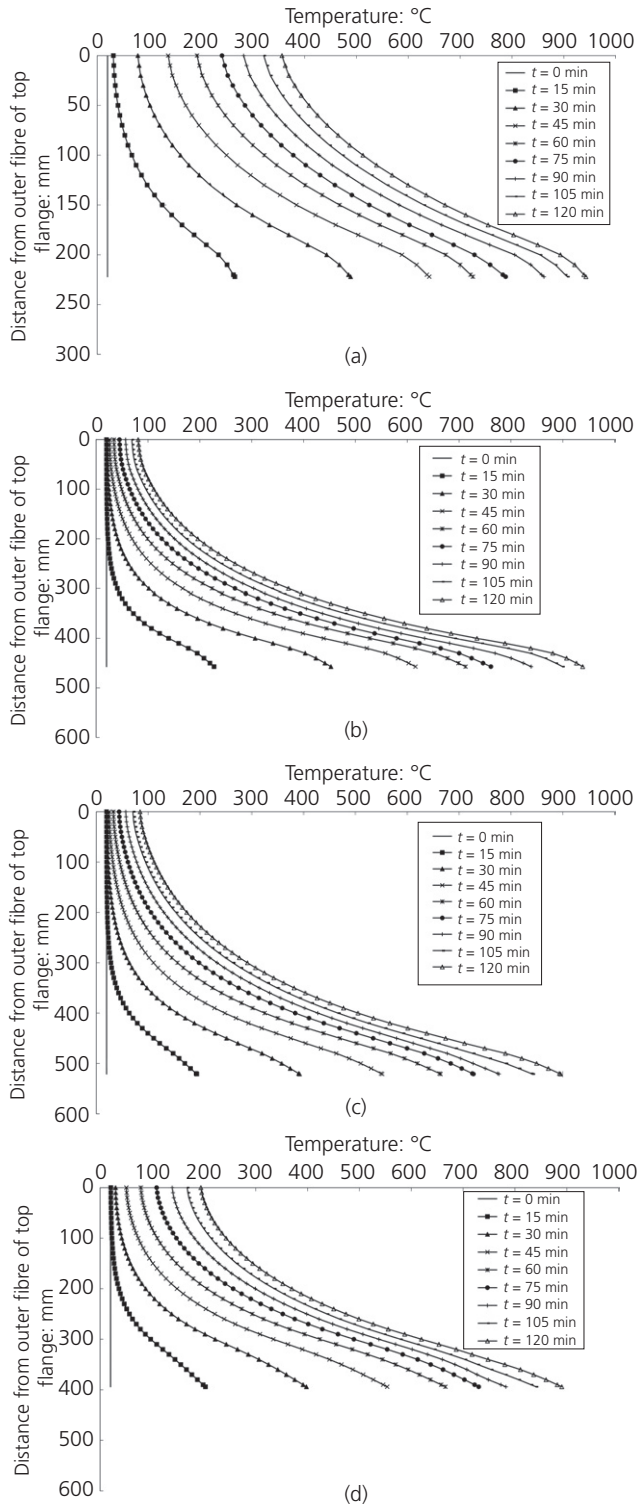


**Figure 8.** Temperature profiles for the cast-iron sections of jack arch beam cross-sections shown in Figure 7: (a) Marshall mill (1817); (b) Armley mill (1823); (c) Shaw’s G mill (1851); (d) Shaw’s H mill (1880)

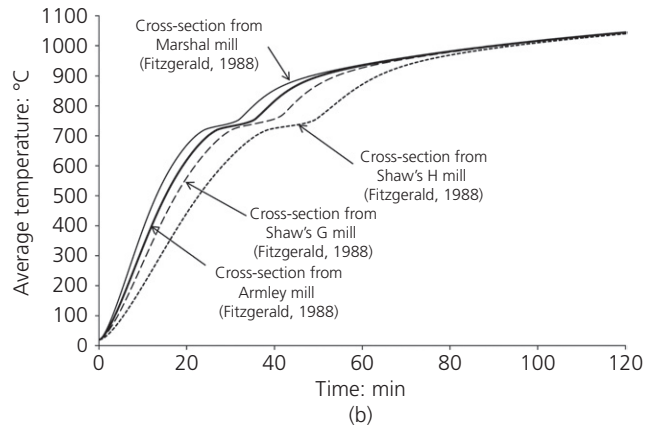
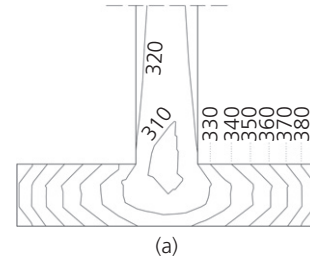


**Figure 9.** (a) Typical temperature distribution (in °C) in the cross-section (Shaw’s H mill, 15 min exposure). (b) Average temperature distributions in unprotected cross-sections

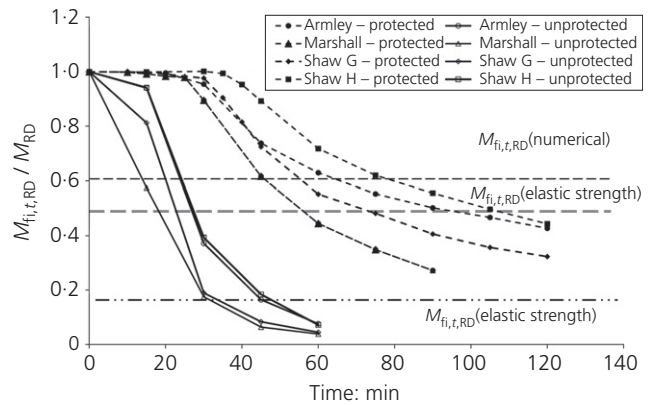


**Figure 10.** Moment capacities of different structures as a function of standard fire exposure time

$$\begin{aligned}
 \varepsilon_{c,T} &= 0.9\varepsilon_{t,20} & 20^\circ\text{C} \leq T \leq 400^\circ\text{C} \\
 \varepsilon_{c,T} &= 0.9\varepsilon_{t,20} \left[ 1 - 0.375 \left( \frac{T - 400}{500} \right) \right] & 400^\circ\text{C} < T \leq 900^\circ\text{C}
 \end{aligned}$$

where  $\varepsilon_{t,20}$  is the strain (0.67% for the material in Figure 5(b)) at peak tensile stress at ambient temperature.

Offprint provided courtesy of www.icevirtualibrary.com  
Author copy for personal use, not for distribution

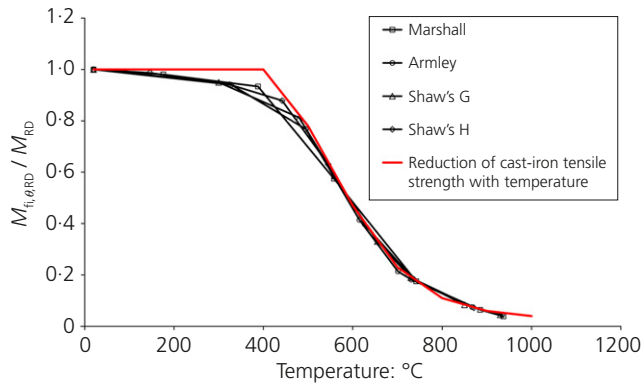


**Figure 11.** Reductions in bending moment capacity of different cast-iron beams with uniform temperature and comparison with cast-iron tensile strength reduction factor

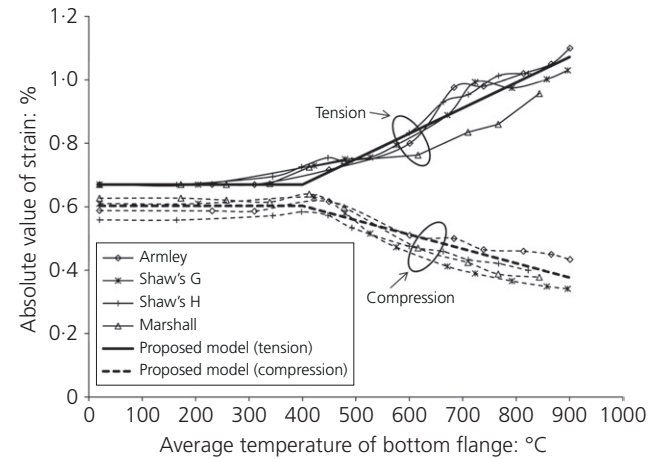


**Figure 13.** Maximum tensile and compressive strains versus average bottom flange temperature

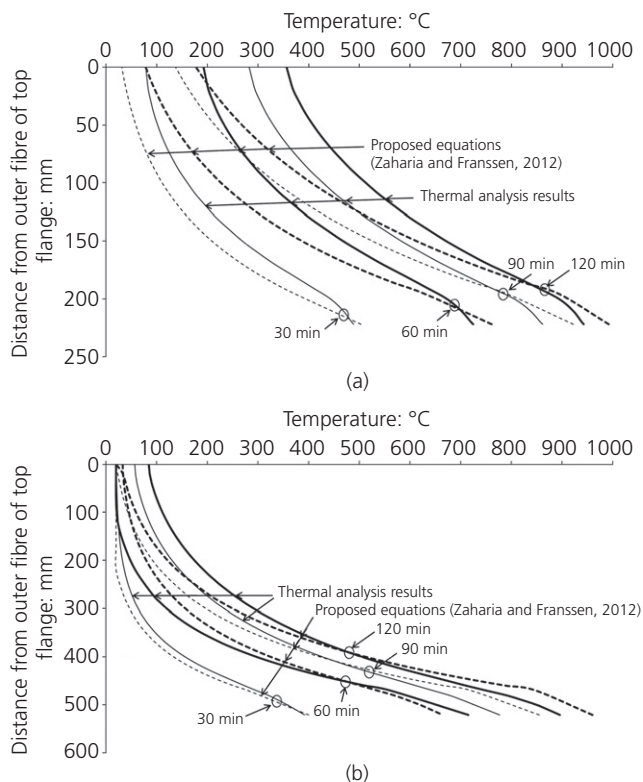


**Figure 12.** Comparison of the temperature profiles obtained by thermal analysis and the equations proposed by Zaharia and Franssen (2012) for: (a) Marshall mill cross-section; (b) Shaw's H cross-section

Based on these assumed maximum tensile and compressive strains, the following simplified method of calculating cast-iron beam bending moment resistance can be suggested (Figure 14).

- The temperature profile of the cast-iron beam cross-section is calculated.
- The 400°C line is determined.
- Based on the average bottom flange temperature, the maximum tensile and compressive strains at the bottom and the top edges of the cross-section, respectively are calculated using Equations 1 and 2, which consequently determines the position of the neutral axis.
- Using the above strain distribution in the cross-section, the stress distribution in the cross-section can be divided into four blocks.

- (i) In block A (tensile stress, temperature > 400°C), the stress distribution may be considered linear between the stress at the lower edge (corresponding to maximum temperature of the cross-section) of the bottom (tensile) flange to the stress at 400°C.
- (ii) Block B represents elastic stress distribution from 400°C in the tensile zone to zero at the neutral axis.
- (iii) In block C, the stress changes from zero at the neutral axis to the compressive yield stress at ambient temperature at a depth  $L_c$  from the top flange.
- (iv) Block D has constant stress.

The depth  $L_c$  is determined by considering equilibrium of tensile and compressive forces. If  $L_c < 0$ , the distribution of the compressive stress is triangular and the maximum compressive stress can be calculated for cross-section equilibrium.

- The bending moment resistance of the cast-iron beam cross-section is the sum of bending moments of all the four zones.

In order to further improve the accuracy of the simplified method, block A may be further divided into smaller zones at 100°C temperature intervals, as shown in Figure 15.

Offprint provided courtesy of www.icevirtuallibrary.com  
 Author copy for personal use, not for distribution

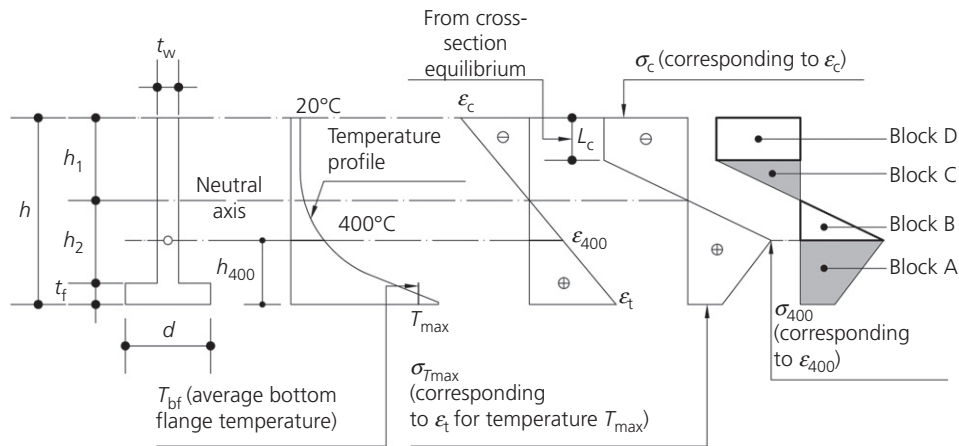


Figure 14. Temperature, strain and stress distributions in cast-iron beam cross-section for proposed simplified model for calculation of the moment capacity of partially protected cast-iron beam

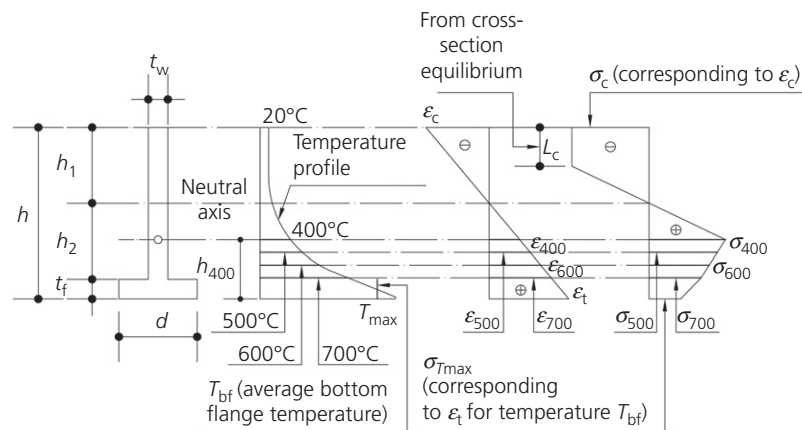


Figure 15. Refined stress distribution in cast-iron beam cross-section

Figure 16 compares the stress profiles obtained from the simplified procedure above and from the fibre analysis model. Appendix 3 uses an example to show the calculation procedure.

The calculation results using the simplified method and using the fibre analysis model are compared in Figure 17. The temperature profiles of the cross-sections used in the simplified method calculations were obtained using thermal analysis and the simplified equations proposed by Zaharia and Franssen (2012). The agreement between these two sets of results is excellent throughout the entire fire exposure for all the different types of cast-iron beams considered.

### 7. Sensitivity analysis

As shown in Figure 13, there are variations between computationally estimated strains and the suggested strain distribution. A sensitivity analysis was thus performed in order to ascertain whether the moment capacity is sensitive to these strain variations. For this purpose, the extreme bounds of maximum strain values shown in Figure 18 were used.

The upper bounds of maximum strains are given by

$$\varepsilon_{t,T} = \varepsilon_{t,20} \quad 20^\circ\text{C} \leq T \leq 300^\circ\text{C}$$

$$\varepsilon_{t,T} = \varepsilon_{t,20} + 0.65 \left( \frac{T - 300}{600} \right) \varepsilon_{t,20} \quad 300^\circ\text{C} < T \leq 900^\circ\text{C}$$

Offprint provided courtesy of www.icevirtuallibrary.com  
 Author copy for personal use, not for distribution

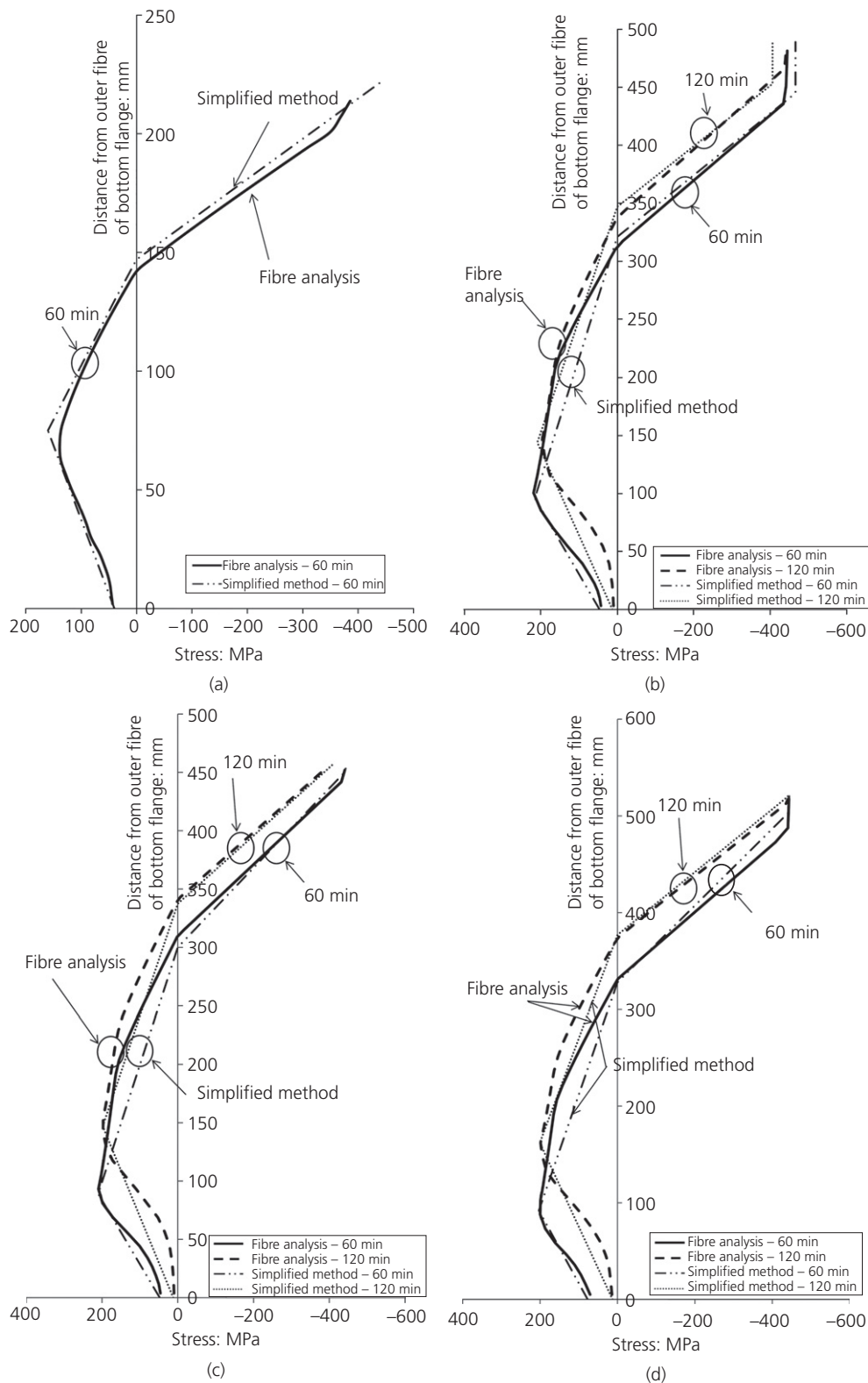


**Figure 16.** Comparison of stress distributions calculated with the fibre model and the simplified method for the sections of Figure 7 ((a) Marshall, (b) Armley, (c) Shaw's G and (d) Shaw's H) for temperature profiles calculated with thermal analysis

Offprint provided courtesy of www.icevirtuallibrary.com  
 Author copy for personal use, not for distribution

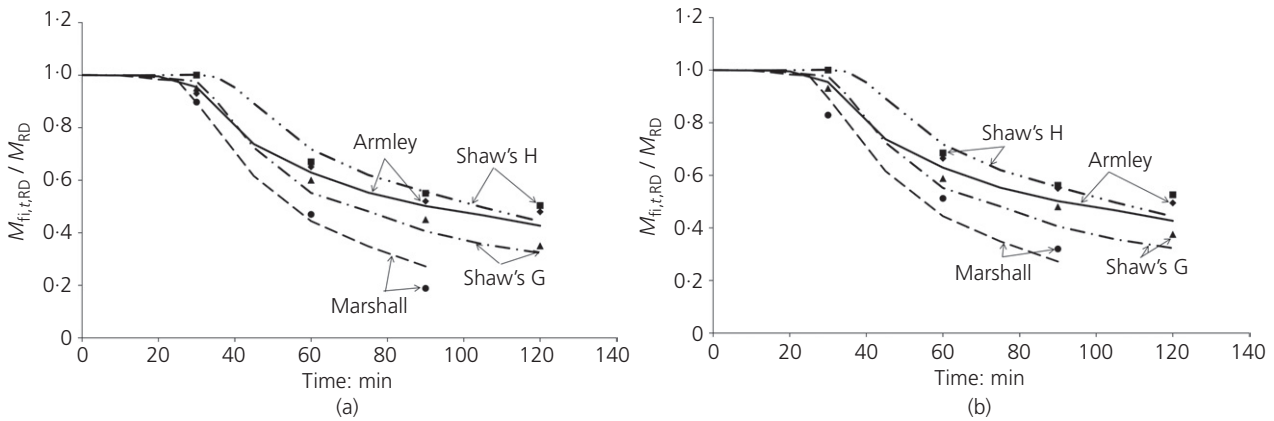


**Figure 17.** Comparison of bending moment resistances obtained with fibre analysis method and simplified method with use of temperature profiles from (a) thermal analysis for both methods and (b) thermal analysis for fibre analysis and simplified

temperature profiles (Zaharia and Franssen, 2012) for simplified moment calculation method. The simplified method results are shown with symbols and the curves represent the fibre analysis results

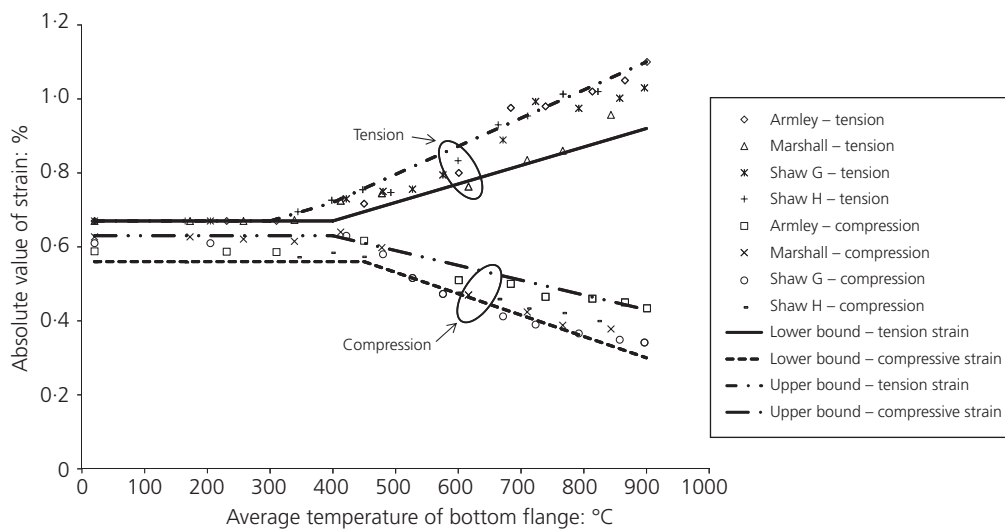


**Figure 18.** Upper and lower strain bounds

$$\epsilon_{c,T} = 0.9\epsilon_{t,20} \quad 20^\circ\text{C} \leq T \leq 400^\circ\text{C}$$

4. 
$$\epsilon_{c,T} = 0.9\epsilon_{t,20} \left[ 1 - \frac{1}{3} \left( \frac{T - 400}{500} \right) \right] \quad 400^\circ\text{C} < T \leq 900^\circ\text{C}$$

$$\epsilon_{c,T} = 0.9\epsilon_{t,20} \quad 20^\circ\text{C} \leq T \leq 450^\circ\text{C}$$

6. 
$$\epsilon_{c,T} = 0.9\epsilon_{t,20} \left[ 1 - 0.5 \left( \frac{T - 450}{450} \right) \right] \quad 450^\circ\text{C} < T \leq 900^\circ\text{C}$$

and the lower bound maximum strains are

$$\epsilon_{t,T} = \epsilon_{t,20} \quad 20^\circ\text{C} \leq T \leq 450^\circ\text{C}$$

5. 
$$\epsilon_{t,T} = \epsilon_{t,20} + 0.37 \left( \frac{T - 450}{450} \right) \epsilon_{t,20} \quad 450^\circ\text{C} < T \leq 900^\circ\text{C}$$

Six analyses were conducted, as shown in Table 1, consisting of the six combinations of the upper and lower bounds and the proposed strain model. Figure 19 compares the fibre analysis results with these six sensitivity results. From these comparisons, it transpires that the maximum difference in bending moment capacities is 8%, which is generally deemed

Offprint provided courtesy of www.icevirtualibrary.com  
Author copy for personal use, not for distribution

	Tensile strain	Compressive strain
Analysis 1	Proposed model (Equation 1)	Upper bound (Equation 4)
Analysis 2	Proposed model (Equation 1)	Lower bound (Equation 6)
Analysis 3	Upper bound (Equation 3)	Proposed model (Equation 2)
Analysis 4	Lower bound (Equation 5)	Proposed model (Equation 2)
Analysis 5	Upper bound (Equation 3)	Lower bound (Equation 6)
Analysis 6	Lower bound (Equation 5)	Upper bound (Equation 4)

**Table 1.** Combinations considered for sensitivity analysis

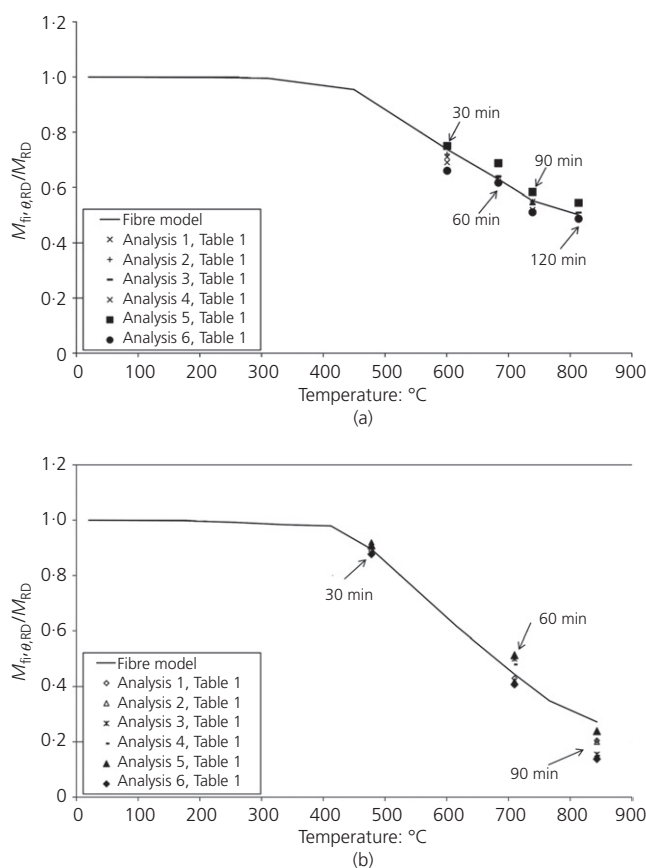


**Figure 19.** Comparison of the simplified calculation method using various maximum strains and the fibre analysis model: (a) Armlay cross-section; (b) Marshall cross-section

satisfactory considering that there are many uncertainties in this type of construction.

## 8. Summary and conclusions

This paper has presented the development and validation of a simplified method to calculate the bending moment resistance of protected and unprotected cast-iron beams exposed to a standard fire condition. In general, jack arched cast-iron beams can achieve 60 min fire resistance (R60) or higher.

Validation of the method was based on comparisons of bending moment capacities calculated using the simplified method and the fibre analysis method. The fibre analysis method was used as a more efficient substitute for finite-element analysis. The differences between these two methods were less than 8%, indicating that the simplified method is an acceptable basis for design.

The simplified method is as follows.

- For unprotected sections, a uniform temperature distribution in the section can be assumed. The bending moment reduction factor is the same as the reduction factor for the tensile strength of cast iron.
- For protected sections, the simplified temperature profiles of Zaharia and Franssen (2012), originally developed for slim floor steel beams, can be used. To calculate the cross-section moment capacity, a strain-based approach can be used.

The procedure of the strain-based approach is as follows.

- The temperature profile of the cast-iron beam cross-section is calculated, based on the approximate solution of Zaharia and Franssen (2012).
- The 400°C line is determined.
- Based on the average bottom flange temperature, the maximum tensile and compressive strains are calculated using Equations 1 and 2. From the strain distribution, the position of the neutral axis can be determined.
- The stress distribution in the cross-section is divided into blocks A, B, C, D, as shown in Figure 14. The stresses at the bottom and top edges are calculated using the above maximum tensile and compressive strains according to the stress–strain–temperature curves in Figure 5(b) (Maraveas *et al.*, 2015). The stress at 400°C is considered to be the same as at ambient temperature. The distance  $L_c$  is obtained from consideration of equilibrium in the cross-section.

The bending moment resistance of the cast-iron beam cross-section is the sum of the bending moments of all the zones (A, B, C, D in Figure 14) of the cross-section.

Offprint provided courtesy of www.icevirtuallibrary.com  
 Author copy for personal use, not for distribution

**Appendix 1 Results of a typical converged iteration of calculation**

The results of a typical converged iteration of calculation are shown in Figure 20.

**Appendix 2 Utilisation factor**

This appendix presents a calculation example for the utilisation factor (the ratio of applied bending moment in fire to the cross-section moment resistance at ambient temperature ( $M_{\text{fibre}}$ )) for the Armley cross-section (Figure 7) with the material properties shown in Figure 5(b).

**A2.1 Moment capacity at ambient temperatures: normal temperature design**

At ambient temperature, the design moment resistance is based on the elastic moment capacity as given by

$$7. \quad M_{\text{el,Rd}} = \frac{W_{\text{el,u}} \times f_y}{\gamma_d}$$

where  $W_{\text{el,u}}$  is the tensile elastic modulus and  $\gamma_d$  is the design safety factor.

For the given cross-section,  $\gamma_d = 3$  and the maximum tensile stress is 219 MPa (Figure 5(b)) or 69.6 MPa according to the London County Council (General Powers) Act 1909 (1909). The calculated elastic moment capacities are, respectively

$$M_{\text{el,Rd}}^{219} = \frac{459.35}{3} \text{ kNm} = 153.12 \text{ kNm}$$

$$M_{\text{el,Rd}}^{69.6} = \frac{145.98}{3} \text{ kNm} = 48.66 \text{ kNm}$$

When using fibre analysis where the non-linear stress distribution is considered, the more accurate value of moment capacity of the cross-section is

$$M_{\text{el,Rd}}^{\text{fibre}} = \frac{602.51}{3} \text{ kNm} = 200.84 \text{ kNm}$$

This gives the following over-strength factors for the Armley cross-section

$$\frac{M_{\text{el,Rd}}^{\text{fibre}}}{M_{\text{el,Rd}}^{219}} = \frac{200.84}{153.12} = 1.31$$

$$\frac{M_{\text{el,Rd}}^{\text{fibre}}}{M_{\text{el,Rd}}^{69.6}} = \frac{200.84}{48.66} = 4.12$$

**A2.2 Utilisation factor for fire design**

Assuming a linear relationship between the applied load and bending moment, the applied bending moment in the fire situation is

$$8. \quad M_{\text{fi}} = M_{\text{el,RD}} \frac{\gamma_{\text{fi}}}{\gamma_d}$$

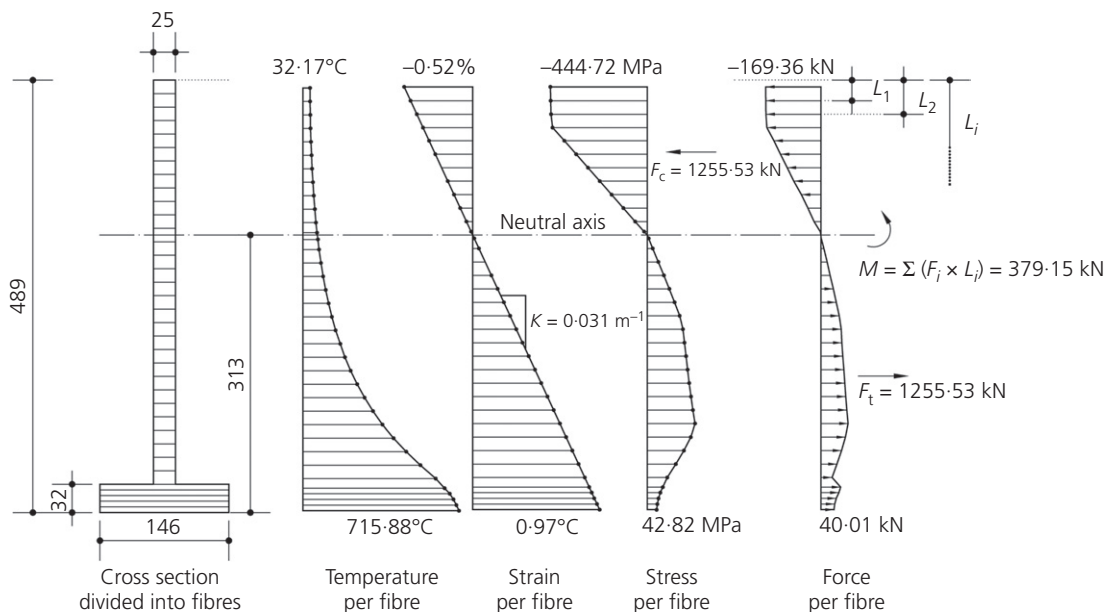


Figure 20. Results of a typical converged iteration of calculation (dimensions in mm)

Offprint provided courtesy of www.icevirtuallibrary.com  
 Author copy for personal use, not for distribution

where  $\gamma_{fi}$  is the safety factor for fire design. Therefore

$$M_{fi} = M_{el,Rd} \frac{2}{3}$$

The utilisation factor can be expressed as

$$9. \quad \mu = \frac{M_{fi}}{M_{fibre}} = \frac{M_{fi}}{M_{el,Rd}} \frac{M_{el,Rd}}{M_{fibre}} = \frac{2}{3} \frac{M_{el,Rd}}{M_{fibre}}$$

For the particular Armley cross-section, the utilisation factors are

$$\mu = \frac{2}{3 \times 1.31} = 0.5$$

for an over-strength ratio of 1.31 and

$$\mu = \frac{2}{3 \times 4.12} = 0.17$$

for an over-strength ratio of 4.12.

**Appendix 3 Calculation example of simplified moment capacity evaluation procedure**

This appendix presents a calculation example for the Armley cross-section (Figure 7) for 60 min of ISO 834 fire exposure.

**A3.1 Temperatures**

From Figure 8(b), the average temperature of the bottom flange is 700°C and the maximum is 722°C and the position with 400°C is 400 mm from the top of the cross-section or 89 mm from the bottom.

**A3.2 Strains**

From Equations 1 and 2, for  $\epsilon_{t,20} = 0.67\%$  the maximum tensile and compression strains for the 700°C bottom flange temperature are

$$\epsilon_t = 0.911\%$$

$$\epsilon_c = 0.467\%$$

For these maximum strains, the position of the neutral axis is 166 mm from the top side of the cross-section and the strain 400°C point is  $\epsilon_{400} = 0.66\%$  (Figure 21).

**A3.3 Stresses**

From the applied stress-strain-temperature relationship (Figure 5(b)) the corresponding stresses are:

$$\sigma_t^{722} = 42.08 \text{ MPa (corresponding to } \epsilon_t)$$

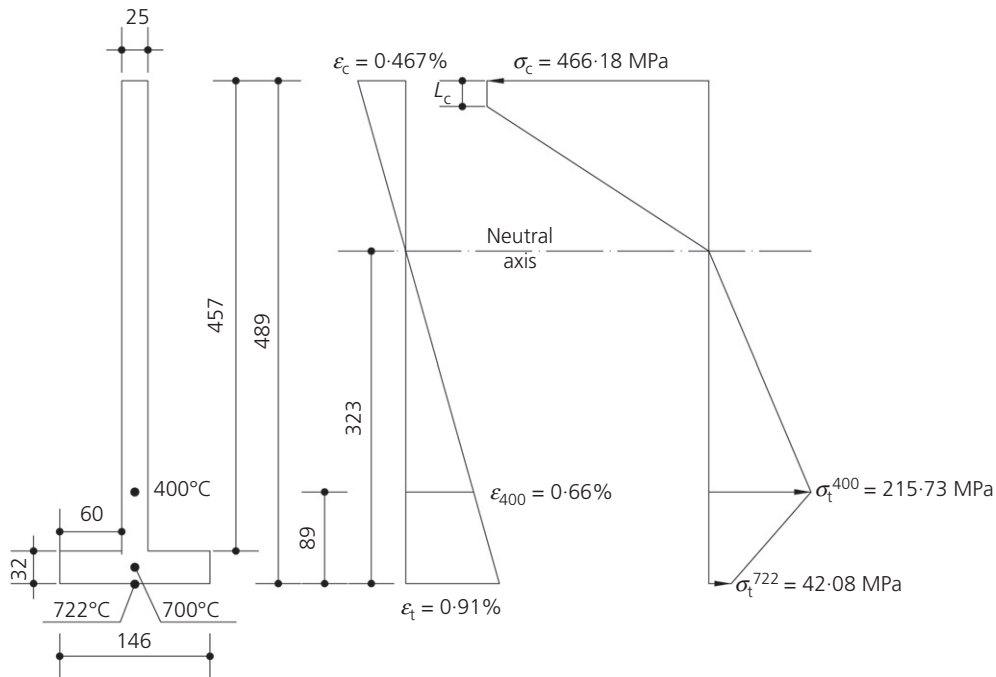


**Figure 21.** Strain-based stresses for the calculation of moment capacity according to the simplified method

Offprint provided courtesy of www.icevirtuallibrary.com  
 Author copy for personal use, not for distribution

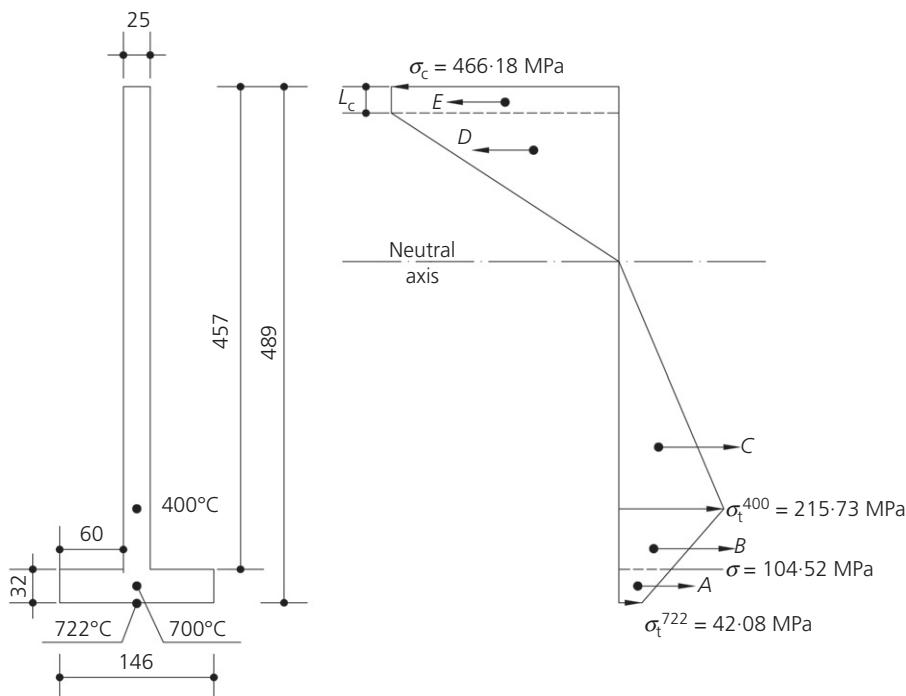


Figure 22. Internal forces

$$\sigma_t^{400} = 215.73 \text{ MPa (corresponding to } \epsilon_{400})$$

$$\sigma_c^{20} = 466.18 \text{ MPa (corresponding to } \epsilon_c)$$

The stress distribution is shown in Figure 21. The stresses result in five internal forces (Figure 22) *A*, *B*, *C*, *D* and *E* applied at the centre of gravity of each stress block. Forces *D* and *E* are functions of  $L_c$ . From cross-section equilibrium, the length  $L_c$  can be calculated as

$$\begin{aligned} \Sigma F_x = 0 \rightarrow A + B + C - D(L_c) - E(L_c) = 0 \rightarrow L_c \\ = 40 \cdot 21 \text{ mm} \end{aligned}$$

So, the internal forces are  $A = 342.4 \text{ kN}$ ,  $B = 228.2 \text{ kN}$ ,  $C = 631.0 \text{ kN}$ ,  $D = 733.07 \text{ kN}$  and  $E = 468.5 \text{ kN}$  (Figure 22). After multiplying each internal force with the appropriate lever arm, the moment capacity can be calculated. For this cross-section and the given temperatures, the moment capacity is

$$M = 391 \cdot 8 \text{ kNm}$$

For comparison, the fibre analysis model gives  $M = 379.15 \text{ kNm}$ .

REFERENCES

Angus TH (1976) *Cast Iron: Physical and Engineering Properties*, 2nd edn. Butterworths, London, UK.

Bodzak P, Kozicki J and Urban T (2014) Investigations of cast iron girders from Manufaktura – former spinning factory in Lodz. *Proceedings of 2nd International Conference on Protection of Historical Constructions, Antalya, Turkey*, pp. 229–234.

Burgess I, El-Rimawi J and Plank R (1988) A secant stiffness approach to the fire analysis of steel beams. *Journal of Constructional Steel Research* **11**: 105–120.

Burgess IW, El-Rimawi JA and Plank RJ (1990) Analysis of beams with non-uniform temperature profile due to fire exposure. *Journal of Constructional Steel Research* **16**: 169–192.

CEN (European Committee for Standardization) (2005a) EN 1993-1-2: Eurocode 3 – design of steel structures – part 1-2: general rules – structural fire design. CEN, Brussels, Belgium.

CEN (2005b) EN 1992-1-2: Eurocode 2 – design of concrete structures – part 1-2: general rules – structural fire design. CEN, Brussels, Belgium.

Clark EV (1901) The theory of cast iron beams. *Proceedings of the Institution of Civil Engineers* **149(1902)**: 313–341.

Fitzgerald R (1988) The development of the cast iron frame in textile mills to 1850. *Industrial Archaeology Review* **X(2)**: 127–145.

Offprint provided courtesy of [www.icevirtuallibrary.com](http://www.icevirtuallibrary.com)  
Author copy for personal use, not for distribution

- Friedman D (1995) Cast-iron-column strength in renovation design. *Journal of Constructed Facilities* **9(3)**: 220–230.
- Hurst G (1990) *The Age of Fireproof Flooring*. The Iron Revolution, London, UK, pp. 35–39.
- ISO (International Organization for Standardization) (1999) ISO 834: Fire resistance tests – elements of building construction – part 1: general requirements. ISO, Geneva, Switzerland.
- IStructE (Institution of Structural Engineers) (1996) *Appraisal of Existing Structures*, 2nd edn. IStructE, London, UK.
- Kattus JR and McPerson B (1959) *Report on Properties of Cast Iron at Elevated Temperatures*. ASTM, West Conshohocken, PA, USA, ASTM STP 248.
- London County Council (General Powers) Act 1909 (1909) *9 Ed VII Cap CXXX*. HMSO, London, UK.
- Maraveas C, Wang YC and Swailes T (2013) Thermal and mechanical properties of 19th century fireproof flooring systems at elevated temperatures. *Construction and Building Materials* **48**: 248–264.
- Maraveas C, Wang YC and Swailes T (2014) Fire resistance of 19th century fireproof flooring systems: a sensitivity analysis. *Construction and Building Materials* **55**: 69–81.
- Maraveas C, Wang YC, Swailes T and Sotiriadis G (2015) An experimental investigation of mechanical properties of structural cast iron at elevated temperatures and after cooling down. *Fire Safety Journal* **71**: 340–352.
- Palmer KB (1970) High temperature properties of cast irons. *Proceedings of Conference on Engineering Performance of Iron Castings*. British Cast Iron Research Association, pp. 217–249.
- Parmenter M (1996) *An Investigation of the Strength of Cast Iron Beams*. PhD thesis, Department of Civil and Structural Engineering, UMIST, Manchester, UK.
- Paulson C, Tide RHR and Meinheit DF (1996) Modern techniques for determining the capacity of cast iron columns. In *Standards for Prevention and Rehabilitation* (Kelley SJ (ed.)). ASTM, West Conshohocken, PA, USA, ASTM STP 1258, pp. 186–200.
- Rondal J and Rasmussen KJR (2003) On the strength of cast iron columns. *Journal of Constructional Steel Research* **60**: 1257–1270.
- Swailes T (2003) 19th century ‘fireproof’ buildings, their strength and robustness. *The Structural Engineer* **81(19)**: 27–34.
- Swailes T (1995) 19th century cast-iron beams: their design, manufacture and reliability. *Proceedings of the Institution of Civil Engineers – Civil Engineering* **114(1)**: 25–35.
- Wermiel S (1993) The development of fireproof construction in Great Britain and the United States in the nineteenth century. *Construction History* **9(1)**: 3–26.
- Zaharia R and Franssen JM (2012) Simple equations for the calculation of the temperature within the cross-section of slim floor beams under ISO fire. *Steel and Composite Structures* **13(2)**: 171–185.

---

#### WHAT DO YOU THINK?

To discuss this paper, please email up to 500 words to the editor at [journals@ice.org.uk](mailto:journals@ice.org.uk). Your contribution will be forwarded to the author(s) for a reply and, if considered appropriate by the editorial panel, will be published as discussion in a future issue of the journal.

*Proceedings* journals rely entirely on contributions sent in by civil engineering professionals, academics and students. Papers should be 2000–5000 words long (briefing papers should be 1000–2000 words long), with adequate illustrations and references. You can submit your paper online via [www.icevirtuallibrary.com/content/journals](http://www.icevirtuallibrary.com/content/journals), where you will also find detailed author guidelines.